# Mechanism of Thermal Aggregation of Rabbit Muscle Glyceraldehyde-3-phosphate Dehydrogenase†

Kira A. Markossian,*,‡ Helen A. Khanova,‡ Sergey Yu. Kleimenov,‡ Dmitrii I. Levitsky,‡,§ Natalia A. Chebotareva,‡ Regina A. Asryants,§ Vladimir I. Muronetz,§,|| Luciano Saso,⊥ Igor K. Yudin,# and Boris I. Kurganov*,‡

*Bach Institute of Biochemistry, Russian Academy of Sciences, Leninsky 33, Moscow 119071, Russia, Belozersky Institute of Physico-Chemical Biology and Faculty of Bioengineering and Bioinformatics, Moscow State University, Moscow 119992, Russia, Department of Human Physiology and Pharmacology Vittorio Erspamer, University of Rome La Sapienza, Italy, and Oil and Gas Research Institute, Russian Academy of Sciences, Gubkina St., 3, Moscow 117971, Russia*

*Received May 30, 2006; Revised Manuscript Received September 10, 2006*

ABSTRACT: Thermal denaturation and aggregation of rabbit muscle glyceraldehyde-3-phosphate dehydrogenase (GAPDH) have been studied using differential scanning calorimetry (DSC), dynamic light scattering (DLS), and analytical ultracentrifugation. The maximum of the protein thermal transition ($T_m$) increased with increasing the protein concentration, suggesting that the denaturation process involves the stage of reversible dissociation of the enzyme tetramer into the oligomeric forms of lesser size. The dissociation of the enzyme tetramer was shown by sedimentation velocity at 45 °C. The DLS data support the mechanism of protein aggregation that involves a stage of the formation of the start aggregates followed by their sticking together. The hydrodynamic radius of the start aggregates remained constant in the temperature interval from 37 to 55 °C and was independent of the protein concentration ($R_{h,0} \approx 21$ nm; 10 mM sodium phosphate, pH 7.5). A strict correlation between thermal aggregation of GAPDH registered by the increase in the light scattering intensity and protein denaturation characterized by DSC has been proved.

The process of protein aggregation has received much consideration due to the discovery that a major part of human degenerative and neurodegenerative diseases is associated with a change in the secondary and/or tertiary structure of a native protein, leading to the formation of protein aggregates with various supramolecular organizations (*1*−*7*).

Mammalian glyceraldehyde-3-phosphate dehydrogenase (GAPDH;[1] EC 1.2.1.12), which is abundant in cells, reveals, besides well-known glycolytic function, several other functions and is involved in some degenerative and neurodegenerative diseases. The potential involvement of GAPDH in neurodegeneration is based on the demonstration that proteins important to the pathogenesis of several neuronal disorders strongly bind GAPDH with high affinity in vitro. GAPDH interacts with the β-amyloid precursor protein and the Huntington protein (*8*, *9*). Tsuchiya et al. (*10*) have demonstrated that GAPDH may be involved in the Lewy body-like cytoplasmic inclusion formation in vivo, probably associated with the apoptotic death pathway. Besides, decrease in the enzyme activity has been reported in human lens with age and in cataract (*11*).

GAPDH is a homotetrameric enzyme consisting of monomers with molecular mass of 36 kDa. The polypeptide chain of GAPDH is folded in two domains, the $NAD^+$-binding and catalytic domains, which are relatively independent (*12*). The structure of rabbit muscle GAPDH shares 91% sequence identity with the human enzyme; human GAPDH is a potential target for the development of antiapoptotic drugs.

Several in vitro studies have been devoted to unfolding, refolding, dissociation, association, and aggregation of GAPDH (*13*−*19*). GAPDH has been used as a target protein to examine the effects of some chaperones (*20*−*25*). The enzyme shows only a limited extent of reactivation after denaturation by GdnHCl, and aggregates, as assessed by the turbidity measurements (*26*). The inactivation of GAPDH during thermal denaturation at 38.5 °C in the pH range of 7.65−8.85 has been compared to its dissociation−aggregation measured by light scattering and to the changes in its secondary structure measured by CD in the far-ultraviolet (*14*). It has been shown that the secondary structure of the enzyme is relatively heat stable, showing change only at pH 8.85. Under these conditions, the enzyme first dissociates within several minutes, probably into dimers, and with prolonged heating it becomes irreversibly aggregated.

Dynamic light scattering (DLS) is widely used to study the kinetics of protein aggregation and allows determining the size of protein aggregates (*27*−*34*). In an earlier paper

† This research was supported by the Russian Foundation for Basic Research (Grants 05-04-48691a and 05-04-48955a and Grant 04-04-81038a for collaborative studies with Byelorussia), Program "Molecular and Cell Biology" of the Presidium of the Russian Academy of Sciences, and grants of INTAS (03-51-4813) and NATO (LST.CLG. 979533).

* To whom correspondence should be addressed. Telephone: (7-495) 952-5641. Fax: (7-495) 954-2732. E-mail: markossian@inbi.ras.ru; boris@kurganov.com.

‡ Bach Institute of Biochemistry.

§ Belozersky Institute of Physico-Chemical Biology.

|| Faculty of Bioengineering and Bioinformatics.

⊥ Department of Human Physiology and Pharmacology Vittorio Erspamer.

# Oil and Gas Research Institute.

[1] Abbreviations: GAPDH, glyceraldehyde-3-phosphate dehydrogenase; DSC, differential scanning calorimetry; DLS, dynamic light scattering.

10.1021/bi0610707 CCC: $33.50 
Published on Web 10/13/2006

we studied the kinetics of thermal aggregation of $\beta_L$-crystallin using DLS (*35*). A new mechanism of protein aggregation involving the stage of the formation of the start aggregates has been proposed. A method of estimation of the size of the start aggregates based on the construction of the light scattering intensity versus the hydrodynamic radius plots has been developed. The main stage of the aggregation process resulting in the formation of large-sized aggregates prone to precipitation is the stage of sticking together of the start aggregates and aggregates of higher order. We also elaborated a method for the estimation of the duration of the lag period over which the formation of the start aggregates takes place.

The goal of the present work was to study the kinetics of thermal aggregation of GAPDH at various temperatures and various protein concentrations by DLS. This protein is of special interest, since, as was shown in the present work, the stage of GAPDH denaturation preceding aggregation proceeds by a dissociative mechanism. One would expect that thermal aggregation of the protein for which denaturation involves dissociation of protein oligomer into the oligomeric forms of lesser size has distinguishing characteristics. Correlation between the thermal aggregation of GAPDH registered by the increase in the light scattering intensity, on the one hand, and protein denaturation characterized by DSC or enzyme inactivation, on the other hand, has been studied.

## EXPERIMENTAL PROCEDURES

*Isolation and Purification of GAPDH.* GAPDH was isolated from rabbit muscles as described by Scopes and Stoter (*36*) with an additional purification step using gel filtration on Sephadex G-100 (superfine). GAPDH concentration was determined spectrophotometrically at 280 nm using the absorption coefficient $A_{cm}^{1\%}$ of 10.6 (*37*).

*GAPDH Assay.* GAPDH activity was measured by monitoring the increase in the absorbance at 340 nm produced by the formation of NADH using a UV 1601 Schimadzu spectrophotometer. The reaction was carried out at 20 °C and was initiated by the addition of 2−6 $\mu$g of the enzyme to the reaction mixture containing 100 mM glycine, 100 mM $KH_2PO_4$, pH 8.9, 5 mM EDTA, 1 mM NAD, and 1 mM glyceraldehyde 3-phosphate. The dehydrogenase activity was 70 units/mg of the protein.

*Thermal Inactivation of GAPDH.* Thermal inactivation of GAPDH was studied at 55 °C in 10 mM $KH_2PO_4$, pH 7.5. The reaction was started by the addition of GAPDH solution (8−50 $\mu$L) to 10 mM potassium phosphate buffer; the volume of the reaction mixture was 1 mL. At fixed time intervals, aliquots were withdrawn to determine the enzymatic activity in the standard mixture.

*Calorimetric Studies.* Thermal denaturation of GAPDH was studied by differential scanning calorimetry (DSC). DSC experiments were performed using a DASM-4M differential scanning microcalorimeter (Institute for Biological Instrumentation, Pushchino, Russia). All measurements were carried out in 10 mM sodium phosphate buffer, pH 7.5. The protein solution was heated at a constant rate of 1 °C/min from 5 to 90 °C and at a constant pressure of 2.2 atm. The reversibility of the thermal transition of GAPDH was tested by checking the reproducibility of the calorimetric trace during the second heating of the sample immediately after cooling. The calorimetric traces of GAPDH were corrected for instrumental background and for possible aggregation artifacts by subtracting the scans obtained from the second heating of the samples. The temperature dependence of the excess heat capacity was further analyzed and plotted using Origin software (MicroCal Inc.).

*Analytical Ultracentrifugation.* Sedimentation velocity experiments were carried out at various temperatures (20, 37, or 45 °C) in a model E analytical ultracentrifuge (Beckman), equipped with absorbance optics, a photoelectric scanner, a monochromator, and a computer on line. A four-hole rotor An-F Ti and 12 mm double sector cells were used. The rotor was preheated at an appropriate temperature in the thermostat before the run. The sedimentation profiles of GAPDH were recorded by measuring the absorbance at 280 nm. All cells were scanning simultaneously. The time interval between scans was 3 min. For digital data acquisitions La-n20-12 PC1 and La-1.5 PCI plates and software specially written by A. G. Zharov (www.ADClab.ru) were used. The sedimentation coefficients were estimated from the differential sedimentation coefficient distribution [$c(s)$ versus $s$] or [$c(s, f/f_0)$ versus $s$] which were analyzed using the SEDFIT program (*38*, *39*). The $c(s)$ analysis was performed with regularization at confidence levels of 0.68 and 0.95 and a floating frictional ratio, time-independent noise, baseline, and meniscus position. The sedimentation coefficients were corrected to solvent density and viscosity (20 °C, water) in the standard way as described earlier (*40*). The $c(s)$ distribution was transformed to the $c(M)$ distribution for the run at 20 °C ($M$ is the molecular mass).

*DLS Studies.* For light scattering measurements the commercial instrument Photocor Complex was used (Photocor Instruments Inc.; www.photocor.com). This instrument allows measuring both dynamic and static light scattering (DLS and SLS) at various scattering angles with a stepper-motor controlled turntable (*41*). A He−Ne laser (Coherent, model 31-2082, 632.8 nm, 10 mW) has been used as a light source. The temperature of the sample cell was controlled by the proportional integral derivative (PID) temperature controller to within ±0.1 °C. A quasi-cross-correlation photon counting system with two photomultiplier tubes was used, which allows increasing accuracy of particle sizing in the range of 0.5−10 nm.

DLS data have been accumulated and analyzed with the multifunctional real-time correlator Photocor-FC that has both logarithmic multiple-tau and linear time-scale modes. DynaLS software (Alango) was used for polydisperse analysis of DLS data. The mean hydrodynamic radius of the particles, $R_h$, was calculated from the Stokes−Einstein equation: $D = k_B T/6\pi\eta R_h$, where $k_B$ is Boltzmann's constant, $T$ is the absolute temperature, and $\eta$ is the shear viscosity of the solvent.

To obtain the DLS results with high-rate temperature scanning, as compared to DSC, a fast thermostat has been developed. Special design of this compact unit allowed simply replacing the standard sample cell holder of the main thermostat of the Photocor Complex setup by the fast thermostat. Fast platinum thermometers with a time constant of 1 s have been used both for temperature control and for real-time monitoring of temperature directly in the sample cell. The fast thermostat is fully controlled with the existing PID controller through the macro procedure of the Photocor

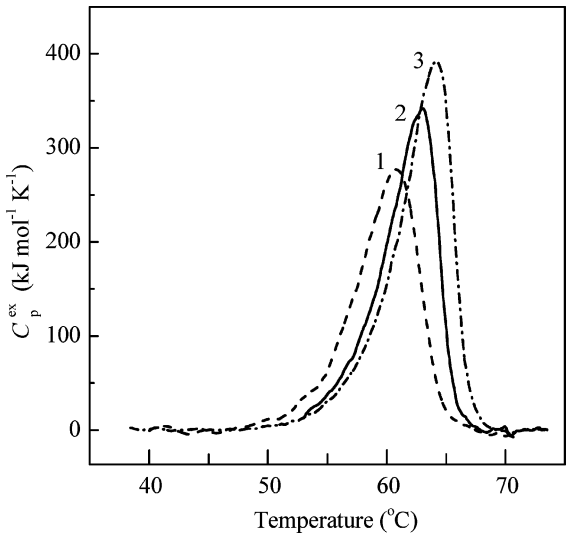


FIGURE 1: Temperature dependences of excess heat capacity ($C_p^{ex}$) of GAPDH (10 mM sodium phosphate buffer, pH 7.5) at various concentrations of the protein: (1) 0.5, (2) 1.5, and (3) 3.0 mg/mL. $C_p^{ex}$ was calculated per GAPDH tetramer. The heating rate was 1 °C/min.

program. The temperature scanning rate can be assigned from 10 °C/min to any slow value. The time of the DLS data accumulation is agreed with the rate of the temperature scanning to obtain correct results of particle sizing in the course of aggregation processes.

The kinetics of thermal aggregation of GAPDH were studied by DLS in 10 mM sodium phosphate buffer, pH 7.5. All solutions for the experiments were prepared using deionized water obtained with the Easy-Pure II RF system (Barnstead). The buffer was placed in a cylindrical cell with the internal diameter of 6.3 mm and preincubated for 10 min at a certain temperature. Cells with stopper were used for incubation at high temperature to avoid evaporation. The aggregation process was initiated by the addition of an aliquot of GAPDH to the final volume of 0.5 mL. When studying the kinetics of aggregation of GAPDH, the scattering light was collected at a 90° scattering angle.

*Calculations*. Origin 7.0 software (OriginLab Corp.) was used for the calculations.

## RESULTS

*Thermal Denaturation of GAPDH.* DSC analysis shows that thermal denaturation of GAPDH is fully irreversible. The heat sorption curve is represented by a sharp thermal transition (Figure 1). The maximum of GAPDH thermal transition ($T_m$) strongly depends on the protein concentration: it increases by 3.5 °C, from 60.7 to 64.2 °C, as the protein concentration rises from 0.5 to 3.0 mg/mL (Figure 1). Such a dependence of $T_m$ on the protein concentration is believed to be characteristic for thermal denaturation of oligomeric proteins and to denote the presence of a stage of reversible dissociation of oligomer into subunits before their irreversible thermal denaturation (*40*, *42*). Indeed, it seems very likely that during heating the tetrameric molecule of GAPDH (the so-called "dimer of dimers") dissociates into dimers (and probably further to monomers) before their irreversible denaturation.

*Analytical Ultracentrifugation of GAPDH.* For testing the oligomeric state of GAPDH during heating, we studied the

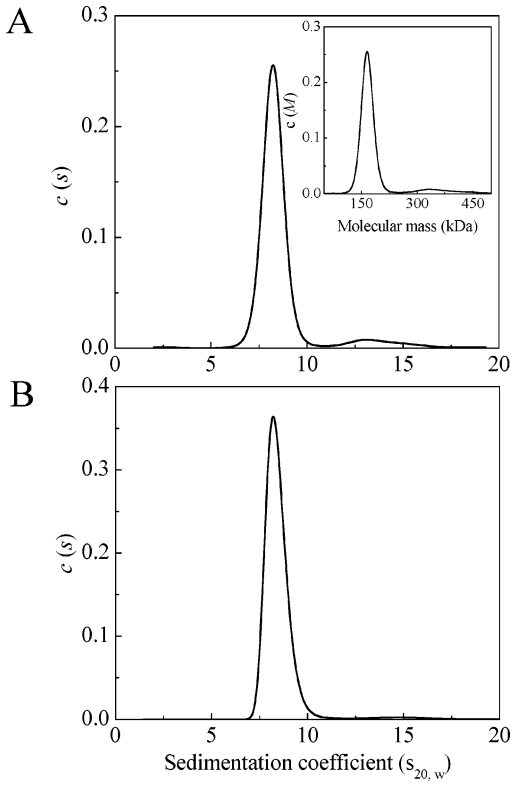


FIGURE 2: Sedimentation behavior of GAPDH (0.4 mg/mL; 10 mM sodium phosphate buffer, pH 7.5). (A) Differential sedimentation coefficient distribution $c(s)$ for GAPDH at 20 °C. The inset shows the $c(M)$ distribution. (B) $c(s)$ distribution for the enzyme preparation heated at 37 °C for 7 h. The $c(s)$ distribution was obtained at 37 °C and normalized to the standard conditions. The rotor speed was 40000 rpm.

sedimentation behavior of the enzyme at elevated temperatures. First of all, we carried out the sedimentation velocity studies of GAPDH at 20 °C (Figure 2A). The major peak in the $c(s)$ distribution with $s_{20,w} = 8.19 \pm 0.49$ S corresponded to the tetrameric form of GAPDH with molecular mass obtained from the $c(M)$ distribution (see inset in Figure 2A) equal to 165 ± 17 kDa. Sedimentation velocity studies of GAPDH at 37 °C showed that the original oligomeric state was retained during a long time. Figure 2B demonstrates one major peak in the differential sedimentation coefficient distribution $c(s)$ for GAPDH preincubated at 37 °C for 7 h. The sedimentation coefficient normalized to the standard conditions ($s_{20,w} = 8.22 \pm 0.53$ S) corresponded to the tetrameric form of GAPDH.

Incubation of GAPDH at 45 °C induced dissociation of the protein (Figure 3). Panels A and B of Figure 3 show that at 80 and 90 min incubation under these conditions the dissociated enzyme forms with the sedimentation coefficients of $s_{20,w} = 3.3$ S ± 0.1 and 5.40 ± 0.08 S, respectively, are observed. It is worthy of note that for the technical reasons the sedimentation analysis does not allow controlling the oligomeric state of GAPDH at the incubation time lesser than 80 min. The $c(s, f/f_0)$ distributions contain the main peak (84% or 79%) with the sedimentation coefficient of $s_{20,w} = 3.3 \pm 0.1$ S (Figure 3A,B) corresponding to the monomeric form and the minor peak (4.3%) with $s_{20,w} = 5.40 \pm 0.08$ S corresponding to the dimeric form of GAPDH. When GAPDH was incubated at 45 °C for a long time (3 and 6 h), the $c(s, f/f_0)$ distributions (Figure 3C,D) contained one major peak (61% or 73%) with $s_{20,w} = 4.9 \pm 0.1$ S corresponding

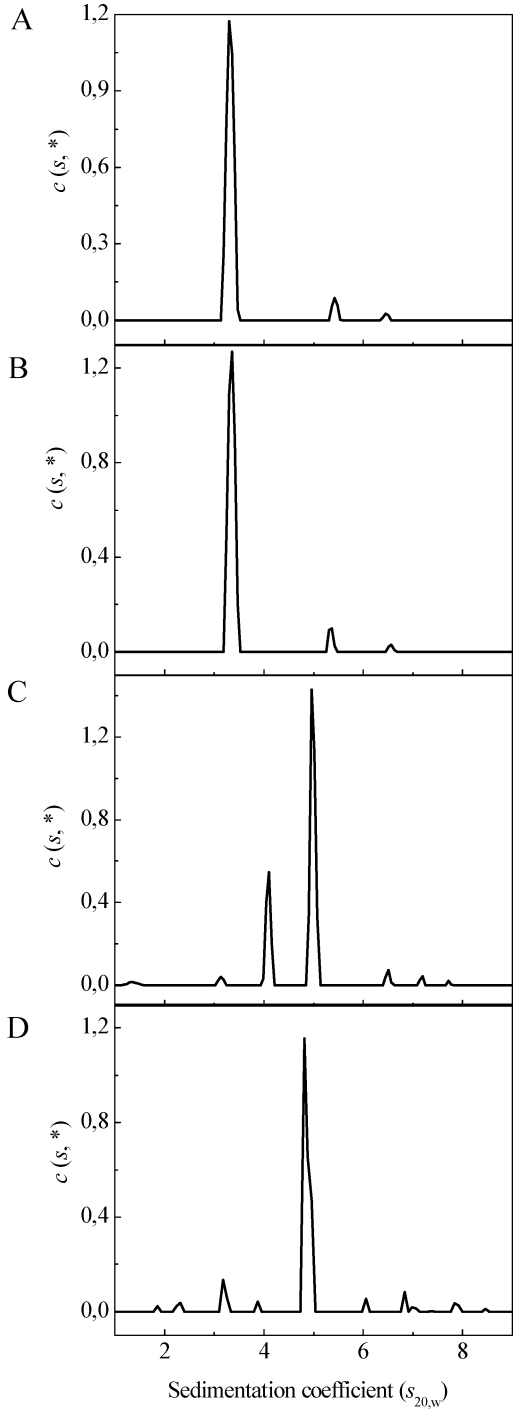


FIGURE 3: Dissociation of GAPDH (0.4 mg/mL) at 45 °C. Differential sedimentation coefficient distributions $c(s, f/f_0)$ for the GAPDH preparation heated at 45 °C for 80 min (A), 90 min (B), 3 h (C), and 6 h (D) were obtained at 45 °C, corrected to the standard conditions, and saved as the one-dimensional $c(s,*)$ distributions. The rotor speed was 30000 rpm.

to the dimeric form. Disappearance of the monomeric enzyme form at longer times of incubation was probably due to association/aggregation of monomers into the dimers.

*Kinetics of Thermal Aggregation of GAPDH.* Thermal aggregation of GAPDH (0.4 mg/mL; 10 mM potassium phosphate, pH 7.5) was studied by DLS in the temperature interval from 37 to 55 °C. DLS allows measuring the hydrodynamic radius ($R_h$) of particles formed in the course of protein aggregation.

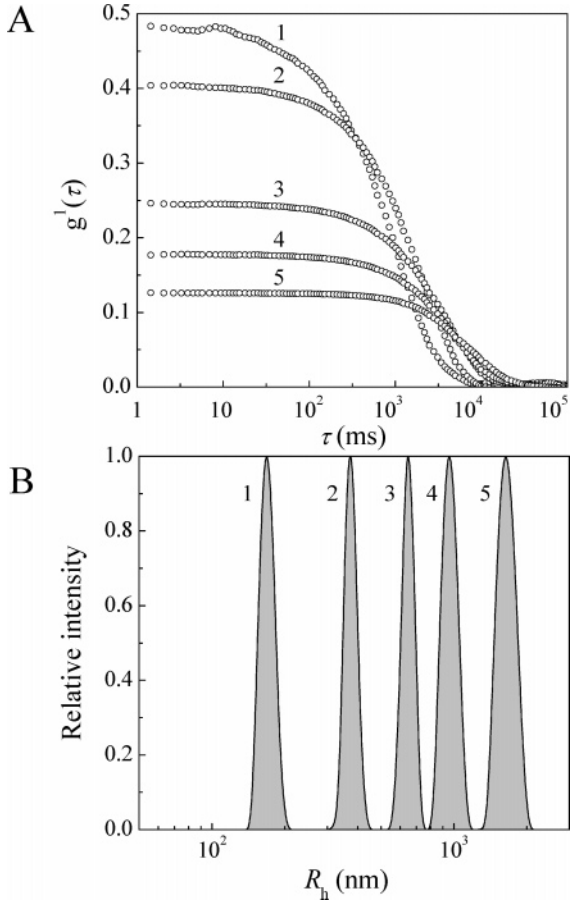


FIGURE 4: Analysis of GAPDH thermal aggregation by DLS. (A) Autocorrelation functions measured at various times of incubation of GAPDH (0.4 mg/mL; 10 mM sodium phosphate buffer, pH 7.5) at 55 °C: (1) 5, (2) 10, (3) 20, (4) 30, and (5) 70 min. (B) Distribution of the particles by their size registered at various times of incubation: (1) 5, (2) 10, (3) 20, (4) 30, and (5) 70 min. DLS measurements were carried out at a scattering angle of 90°.

Figure 4A shows the autocorrelation functions measured at various times of incubation of GAPDH at 55 °C. The distribution of protein aggregates by size obtained at various times of incubation is represented in Figure 4B. As seen, the distribution of aggregates by size is unimodal, and the mean value of the aggregate size changes toward higher $R_h$ values with increasing the incubation time.

Figure 5 shows the dependences of the light scattering intensity and hydrodynamic radius on time (panels A and B, respectively) obtained at various temperatures. As seen from Figure 5A, a lag period is observed in the kinetic curves of the light scattering intensity enhancement. At rather high temperature (55 °C) the dependence of the light scattering intensity on time passes through a maximum. The decrease in the light scattering intensity at high values of time is due to the precipitation of the large-sized aggregates.

Figure 5C shows the dependences of the light scattering intensity on the hydrodynamic radius ($R_h$) obtained at various temperatures. When constructing these dependences, we used the initial values of the hydrodynamic radius corresponding to the region where $R_h$ is a linear function of time (see the inset in Figure 5B). The dependences of the light scattering intensity on $R_h$ are linear and the length cut off on the abscissa axis by the straight line characterizes the size of the start aggregates, i.e., the size of the aggregates that are

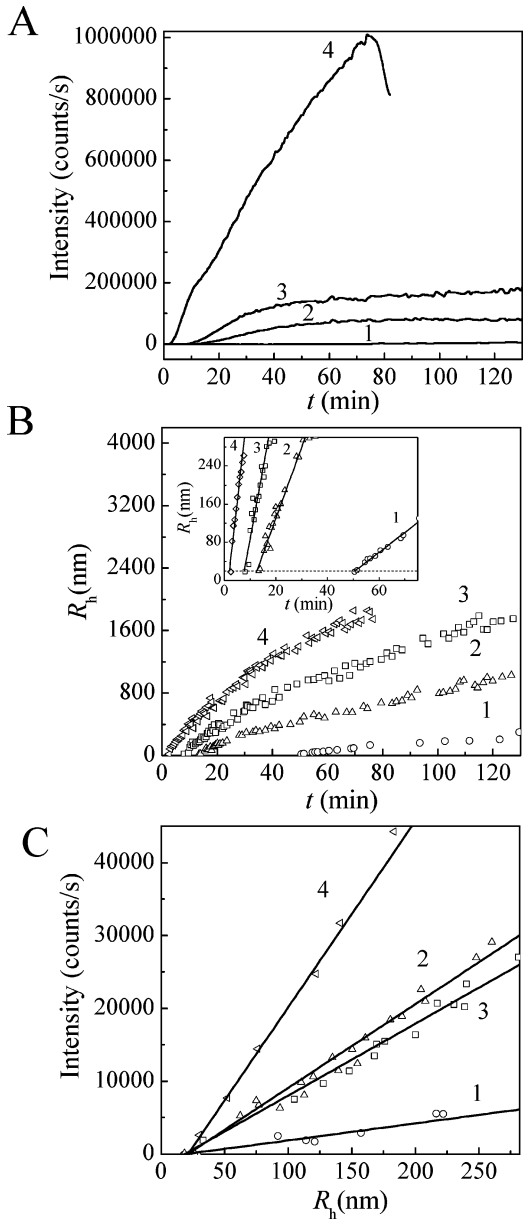


FIGURE 5: Kinetics of thermal aggregation of GAPDH (0.4 mg/mL) at various temperatures: (1) 37, (2) 45, (3) 47.5, and (4) 55 °C. Dependences of the light scattering intensity and $R_h$ on time (panels A and B, respectively). The inset in panel B shows the initial parts of the dependences of $R_h$ on time. The horizontal dotted line corresponds to the $R_{h,0}$ value ($R_{h,0} = 20$ nm). (C) Dependences of the light scattering intensity on $R_h$.

Table 1: Parameters of Equation 1 Used for Description of the Dependences of $R_h$ on Time for Aggregation of GAPDH (0.4 mg/mL)

| temp, °C | $R_{h,0}$, nm | $t_0$, min | $t_{2R}$, min |
|---|---|---|---|
| 37 | 19.5 ± 1.5 | 50.5 ± 0.5 | 4.7 ± 0.2 |
| 45 | 20.2 ± 1.4 | 12.6 ± 0.4 | 1.33 ± 0.05 |
| 47.5 | 19.1 ± 1.2 | 7.6 ± 0.4 | 0.64 ± 0.04 |
| 55 | 21.2 ± 0.8 | 2.0 ± 0.2 | 0.44 ± 0.02 |

registered at the instant an initial increase in the light scattering intensity is observed (see ref *35*). The hydrodynamic radius of the start aggregates ($R_{h,0}$) remains practically constant in the interval of temperatures from 37 to 55 °C (see Table 1). The average value of $R_{h,0}$ was found to be 20.0 ± 1.2 nm. The rough estimation of the number of the denatured monomers of GAPDH in the start aggregates may be performed using an empiric relationship between the molecular mass ($M_r$, kDa) and hydrodynamic radius ($R_h$, nm) of the protein: $M_r = (1.68R_h)^{2.3398}$ (*43*). We assume that this equation is valid only for the stages of aggregation preceding the formation of the start aggregates or involving the formation of the start aggregates by themselves. If we take into account that the molecular mass of the polypeptide chain of GAPDH is 36 kDa, the start aggregate with $R_{h,0} = 20.0 \pm 1.2$ nm should contain approximately 100 ± 20 denatured monomers of GAPDH.

As seen from the inset in Figure 5B, the initial parts of the dependences of $R_h$ on time are linear. The following equation is used for analysis of the initial parts of the dependence of $R_h$ on time:

$$R_h = R_{h,0}\left[1 + \frac{1}{t_{2R}}(t - t_0)\right] \quad (1)$$

where $t_0$ is the duration of the latent stage leading to the formation of the start aggregates and $t_{2R}$ is the time interval over which the hydrodynamic radius increases from $R_{h,0}$ to double this value. The parameter $t_{2R}$ characterizes the rate of aggregation. The lower the $t_{2R}$ value, the higher the aggregation rate. The dotted horizontal line in the inset in Figure 5B corresponds to the $R_{h,0}$ value. The parameter $t_0$ is the length cut off on the horizontal line by the straight line. Parameters of eq 1 ($t_0$ and $t_{2R}$) calculated at various temperatures are given in Table 1. The parameter $t_0$ decreases from 50.5 to 2 min as the temperature rises in the interval of 37−55 °C. In this temperature interval a 10-fold decrease in parameter $t_{2R}$ takes place.

We studied the effect of the protein concentration on the kinetics of thermal aggregation of GAPDH at 55 °C. The dependences of the light scattering intensity and hydrodynamic radius on time obtained at various GAPDH concentrations (0.05−0.4 mg/mL) are presented in Figure 6A,B. The dependences of the light scattering intensity on $R_h$ remain linear at variation of the protein concentration (Figure 6C). The hydrodynamic radius of the start aggregates ($R_{h,0}$) is independent of the protein concentration (Table 2). The average value of $R_{h,0}$ was found to be 22.0 ± 1.2 nm.

With a knowledge of parameter $R_{h,0}$ we can calculate the duration of the latent period resulting in the formation of the start aggregates (see the inset in Figure 6B). The similar values of parameter $t_0$ were obtained at relatively low concentrations of GAPDH (0.05 and 0.2 mg/mL), namely, 8.5 and 10.0 min, respectively (Table 2). Further increase in GAPDH concentration brings about the diminishing of the $t_0$ value ($t_0 = 2.0$ at GAPDH concentration equal to 0.4 mg/mL).

The analysis of the dependences of $R_h$ on time shows that the linear relationship is obeyed up to a certain point in time designated as $t^*$. From this time on, the dependence of $R_h$ on time follows the power law:

$$R_h = R_h^*[1 + K_1(t - t^*)]^{1/d_f} \quad (2)$$

where $R_h^*$ is the value of $R_h$ at $t = t^*$, $K_1$ is a constant, and $d_f$ is the fractal dimension.

This equation is equivalent to the dependence of $R_h$ on time which is obeyed for the diffusion-limited regime of aggregation, i.e., the regime wherein the rate of aggregation

Table 2: Parameters of Equations 1 and 2 Used for Description of the Dependences of $R_h$ on Time for Aggregation of GAPDH at 55 °C

| GAPDH concn, mg/mL | $R_{h,0}$, nm | $t_0$, min | $t_{2R}$, min | $t^*$, min | $R_h^*$, nm | $K_1$, min$^{-1}$ | $d_f$ |
|---|---|---|---|---|---|---|---|
| 0.05 | 22.9 ± 1.5 | 8.5 ± 0.2 | 5.24 ± 0.09 | 22 | 82 | 0.14 ± 0.01 | 1.80 ± 0.05 |
| 0.2 | 22.0 ± 1.5 | 10.0 ± 0.2 | 3.34 ± 0.03 | 21 | 96 | 0.18 ± 0.01 | 1.78 ± 0.04 |
| 0.3 | 23.2 ± 0.8 | 3.5 ± 0.3 | 3.40 ± 0.06 | 18 | 110 | 0.20 ± 0.02 | 1.80 ± 0.05 |
| 0.4 | 21.2 ± 0.8 | 2.0 ± 0.2 | 0.44 ± 0.02 | 10.3 | 348 | 0.27 ± 0.02 | 1.77 ± 0.05 |

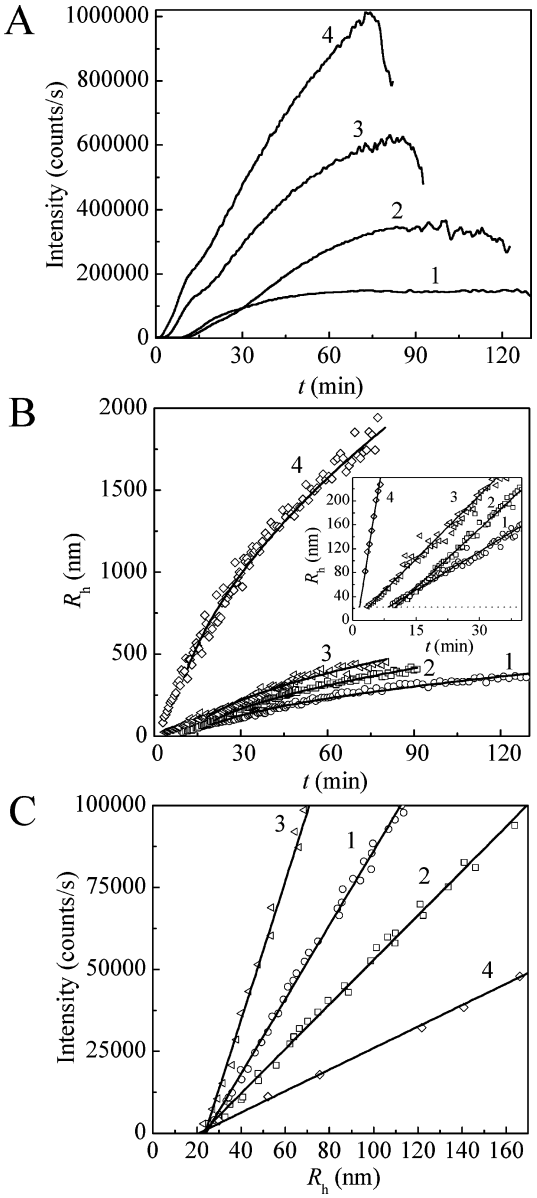


FIGURE 6: Kinetics of thermal aggregation of GAPDH at 55 °C. Dependences of the light scattering intensity on time (A), dependences of $R_h$ on time (B), and dependences of the light scattering intensity on $R_h$ (C) obtained at various concentrations of the enzyme: (1) 0.05, (2) 0.2, (3) 0.3, and (4) 0.4 mg/mL. The inset in panel B shows the initial parts of the dependences of $R_h$ on time. The horizontal dotted line corresponds to the $R_{h,0}$ value ($R_{h,0}$ = 22 nm).

is limited by diffusion of the colliding particles (*44*−*46*):

$$R_h = R_{h,0}(1 + K_1 t)^{1/d_f} \quad (3)$$

where $R_{h,0}$ is the hydrodynamic radius of a seed particle, $d_f$ is the fractal dimension, and $K_1$ is a constant. The fractal dimension is a structural characteristic of aggregates that are

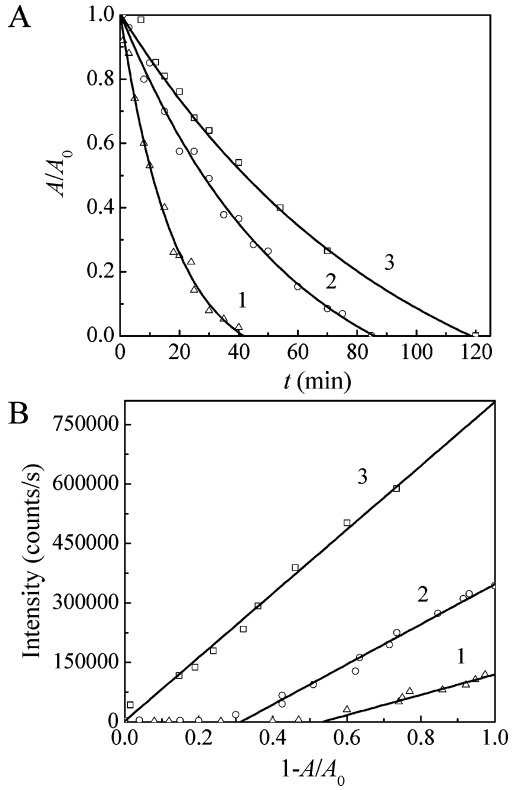


FIGURE 7: Correlation between thermal inactivation and aggregation of GAPDH at 55 °C. (A) Dependences of the relative enzymatic activity $A/A_0$ on time ($A_0$ and $A$ are the initial and current enzymatic activities). (B) Light scattering intensity versus ($1 - A/A_0$) plots. Concentrations of GAPDH were (1) 0.05, (2) 0.2, and (3) 0.3 mg/mL.

formed as a result of unordered interactions (random aggregation). The mass of an aggregate formed in such a way ($M$) is connected with its effective radius ($R$) by the following relationship: $M \sim R^{d_f}$. For aggregation proceeding in the regime of diffusion-limited cluster−cluster aggregation, a universal fractal dimension of 1.8 is observed (*44*−*47*).

The experimental dependences of $R_h$ on time obtained at various concentrations of GAPDH (Figure 6B) were analyzed using eq 2. Parameters obtained ($t^*$, $R_h^*$, and $d_f$) are given in Table 2. The values of $d_f$ are close to the universal value of the fractal dimension ($d_f \approx 1.8$).

*Correlation between Thermal Inactivation and Aggregation of GAPDH.* Figure 7A shows the kinetics of thermal inactivation of GAPDH at 55 °C. The dependences of the relative enzymatic activity $A/A_0$ on time were obtained at various concentrations of the enzyme (0.05, 0.2, and 0.3 mg/mL). As seen from this figure, the rate of inactivation decreases with increasing the enzyme concentration. The time of half-conversion ($t_{0.5}$) increases from 10.9 to 43.1 min, as GAPDH concentration rises from 0.05 to 0.3 mg/mL.

We correlate the increase in the light scattering intensity during GAPDH aggregation at 55 °C with the diminishing

of the enzyme activity. Figure 7B shows the light scattering intensity versus $(1 - A/A_0)$ plots. The $(1 - A/A_0)$ value corresponds to the portion of the inactivated enzyme. When GAPDH concentration was 0.05 mg/mL, the light scattering intensity began to rise at $(1 - A/A_0) > 0.53$. The dependence of the light scattering intensity on $(1 - A/A_0)$ was linear in the interval of the $(1 - A/A_0)$ values from 0.53 to 1.0. When GAPDH concentration was 0.2 mg/mL, the dependence of the light scattering intensity on $(1 - A/A_0)$ was linear in the interval of the $(1 - A/A_0)$ values from 0.31 to 1.0. As GAPDH concentration increased to 0.3 mg/mL, the discordance between the initial increase of the light scattering intensity and the initial decrease in the enzymatic activity disappeared. A strict correlation is observed between aggregation monitored by enhancement of the light scattering intensity and the enzyme inactivation registered by diminishing of the enzyme activity.

*Correlation between Thermal Denaturation and Aggregation of GAPDH*. To substantiate a correlation between thermal denaturation and aggregation of GAPDH, we studied denaturation and aggregation of the enzyme under identical conditions, wherein the temperature was elevated at a constant rate (1 °C/min). On the basis of the DSC data presented in Figure 1 we constructed the $Q/Q_t$ ratio ($Q_t$ is the total heat of denaturation and $Q$ is the heat absorbed, when the certain temperature is achieved) versus temperature plot for GAPDH concentration of 0.5 mg/mL (Figure 8A). $Q_t$ is the area under the whole $C_p^{ex}$ versus temperature profile and $Q$ is the area under the part of profile limited by certain temperature. The $Q/Q_t$ ratio may be considered as a measure of the portion of the denatured protein.

Figure 8B shows the dependence of the light scattering intensity at 632.8 nm on temperature for aggregation of GAPDH (0.5 mg/mL) heated with the constant rate (1 °C/min). The decrease in the light scattering intensity at temperature above 65 °C is due to precipitation of the large-sized aggregates of GAPDH.

Since the dependences of the $Q/Q_t$ ratio and light scattering intensity on temperature were obtained under the same conditions, we can analyze the relationship between the denaturation and aggregation of the enzyme. As seen from Figure 8C, there is a strict correlation between the light scattering intensity and the $Q/Q_t$ ratio characterizing GAPDH aggregation and denaturation, respectively. The length cut off on the ordinate axis at the $Q/Q_t = 1$ by the linear dependence of the light scattering intensity on $Q/Q_t$ gives the limiting value of the light scattering intensity that would be achieved if precipitation would be lacking ($I_{lim} = 148000$ counts/s). It should be noted that there is some discrepancy between the light scattering intensity and the $Q/Q_t$ value in the initial stages of denaturation and aggregation. At $Q/Q_t = 0$ the light scattering intensity has a nonzero value. The reason for this discrepancy is still obscure.

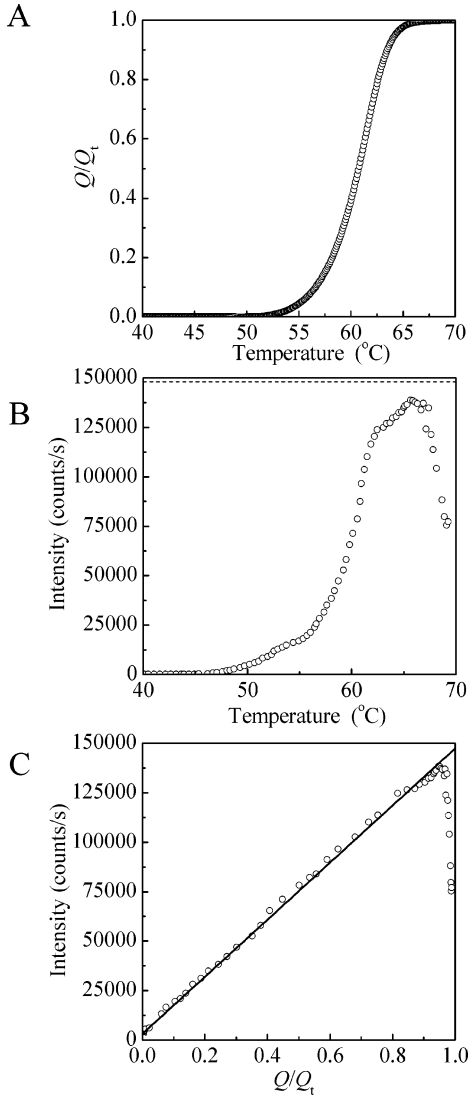


FIGURE 8: Correlation between thermal denaturation and aggregation of GAPDH (0.5 mg/mL). (A) Dependence of the $Q/Q_t$ ratio ($Q_t$ is the total heat of denaturation and $Q$ is the heat absorbed by the time, when the certain temperature is achieved) on temperature calculated from DSC data (Figure 1, curve 1). (B) Dependence of the light scattering intensity at 632.8 nm on temperature for aggregation of GAPDH (0.5 mg/mL) heated with the constant rate (1 °C/min). The horizontal dotted line corresponds to the limiting value of the light scattering intensity, which would be achieved, if precipitation is lacking. (C) Light scattering intensity versus the $Q/Q_t$ ratio plot.

## DISCUSSION

The DSC data on thermal denaturation of GAPDH have shown that the temperature, at which $C_p^{ex}$ reached the maximum value ($T_m$), was shifted toward higher temperatures as GAPDH concentration rose (Figure 1). Such a dependence of $T_m$ on the protein concentration suggests that the overall mechanism of GAPDH denaturation involves stages of reversible dissociation of the enzyme tetramer into the more labile oligomeric forms of lesser size (*40*, *48*−*50*). Sedimentation velocity analysis (Figure 3) also indicates that GAPDH denaturation proceeds by a dissociative mechanism. Panels A and B of Figure 3 show that at 80 and 90 min incubation at 45 °C dissociated enzyme forms with the sedimentation coefficients of $s_{20,w} = 3.3$ S ± 0.1 and 5.40 ± 0.08 S are observed. The main forms (3.3 S) may correspond to the monomer. Increase in the incubation time (3 or 6 h) resulted in the transition of 3.3 S into 4.9 S forms corresponding to dimer. It should be noted that dimers with $s_{20,w} = 5.40 \pm 0.08$ S (Figure 3A,B) and $s_{20,w} = 5.0 \pm 0.1$ S (Figure 3C,D) differ by conformation. The studies of the sedimentation behavior of GAPDH at elevated temperatures (Figure 3) as well as the fact that dilution of GAPDH results in acceleration of the enzyme inactivation (Figure 5A; see

also ref *51*) substantiate the dissociative mechanism of GAPDH denaturation. This mechanism of thermal denaturation has been also shown for other oligomeric proteins (*52*).

When analyzing the data on the kinetics of protein aggregation by DLS, we have proposed to construct the light scattering intensity versus hydrodynamic radius ($R_h$) plots in addition to the usual dependences of the light scattering intensity or $R_h$ on time (*35*, *53*). The shape of the light scattering intensity versus $R_h$ plots directly indicates that the initial stage of thermal aggregation of proteins is the stage of the formation of the start aggregates. The linear character of these plots provides a simple way of estimating the size of the start aggregates.

Using the light scattering intensity versus $R_h$ plots, we have estimated the hydrodynamic radius of the start aggregates formed in the course of thermal aggregation of GAPDH. The $R_{h,0}$ value remained practically constant in the temperature interval from 37 to 55 °C ($R_{h,0} = 20.0 \pm 1.2$ nm). It is worthy of note that the $R_{h,0}$ value was independent of the protein concentration. We observed such a regularity for thermal aggregation of $\beta_L$-crystallin, yeast alcohol dehydrogenase I, rabbit skeletal muscle glycogen phosphorylase *b*, and coat protein of tobacco mosaic virus (*35*, *53*). The character of the change in the slope of the light scattering intensity versus $R_h$ plots at variation of the protein concentration is worthy of special attention. In the case of $\beta_L$-crystallin (*35*) and rabbit skeletal muscle glycogen phosphorylase *b* (*53*) the slope of the light scattering intensity versus $R_h$ plot increases monotonously with increasing protein concentration, whereas regularity is lacking in the arrangement of the dependences of the light scattering intensity on $R_h$ obtained at various concentrations of GAPDH (Figure 6C). If we fix the value of $R_h$, the level of the light scattering intensity corresponding to this $R_h$ value characterizes unambiguously the amount of the aggregated protein. The higher the light scattering intensity, the higher the amount of the aggregated protein. The decrease in the slope of the light scattering intensity versus $R_h$ plot when the GAPDH concentration increases from 0.05 mg/mL (line 1) to 0.2 mg/mL (line 2) or from 0.3 mg/mL (line 3) to 0.4 mg/mL (line 4) is unexpected. The complicated character of the change in the slope of the light scattering intensity versus $R_h$ plot at variation of the GAPDH concentration is due to the fact that GAPDH denaturation preceding aggregation involves the stages of reversible dissociation of the enzyme tetramer into the oligomeric forms of lesser size which are sensitive to variation of the protein concentration. The increase in the GAPDH concentration should interfere with tetramer dissociation and under certain conditions result in the decrease in the amount of the aggregated protein. The attempt to describe accurately the effect of the GAPDH concentration on the slope of the light scattering intensity versus $R_h$ plot is complicated by many things, among them the necessity of taking into account dissociation of the GAPDH tetramer and the transient character of dissociation, denaturation, and aggregation processes. As for the change in the slope of the light scattering intensity versus $R_h$ plots at variation of temperature, the trend has been toward higher slope with increasing temperature (Figure 5C). The higher value of the light scattering intensity at any fixed value $R_h$ at higher temperature is indicative of higher amount of the aggregated protein. The reason is that an increase in temperature results in the enhancement of the rate denaturation with a consequent increase in the amount of the start aggregates and then the amount of the aggregated protein with the selected value of $R_h$. Violation of monotonous increase in the slope of the light scattering intensity versus $R_h$ plot in the region 45−47.5 °C may be also due to the complex mechanism of GAPDH denaturation involving the stages of dissociation of the enzyme oligomer.

Another peculiarity of the aggregation behavior of GAPDH connected with instability of tetrameric structure at elevated temperatures is the change in the shape of the relationship between the light scattering intensity characterizing the aggregation process and the degree of thermal inactivation of GAPDH at variation of the enzyme concentration (Figure 7). Acceleration of inactivation at lower enzyme concentrations results in the lengthening of the part of the $(1 - A/A_0)$ axis where the increment of the light scattering intensity is yet lacking.

When studying thermal aggregation of $\beta$-lactoglobulin at pH 7.0 by size exclusion chromatography, Durand et al. (*54*−*58*) showed that there was a clear separation between a narrow peak that corresponded to residual native protein and a broad peak that corresponded to the aggregates. This observation implied that the aggregates of the minimum size contained many monomers and that no or very few stable oligomers were formed. The authors supposed that the first stage of thermal aggregation of $\beta$-lactoglobulin was the step of the formation of "primary aggregates". The size of the primary aggregates was independent of the protein concentration. It has been shown that sticking together of the primary aggregates was suppressed at low ionic strength due to repulsive interactions. Although the primary aggregates postulated in the works of Durand et al. were formed mainly by intermolecular disulfide bonds (in pH range 6.4−8.0), such aggregates were evidently similar to the start aggregates we observed for $\beta_L$-crystallin and other proteins (*35*, *53*).

On the basis of the data of Durand et al. (*56*) on the sensitivity of sticking of the primary aggregates to variation of ionic strength, one can assume that the start aggregates may be sufficiently stable at low values of ionic strength. From this point of view it is of interest to discuss the properties of the so-called inactivated actin. Turoverov et al. (*59*) observed that 60 min incubation of rabbit skeletal muscle actin (5 mM Tris-HCl, pH 8.2) at 60 °C resulted in the formation of relatively stable particles with an average sedimentation coefficient of 20 S (inactivated actin). The size of the particles of inactivated actin was independent of the protein concentration (within the limits 0.05−1.0 mg/mL). A dramatic increase in 1-anilinonaphthalene-8-sulfonate binding to inactivated actin in comparison with native and unfolded protein indicated that the inactivated actin had solvent-exposed hydrophobic clusters on the surface. In our opinion inactivated actin may be considered as a "frozen" start aggregate.

The fact that at relatively high values of time ($t > t^*$) the dependence of the hydrodynamic radius of GAPDH aggregates on time follows the power law with $d_f \approx 1.8$ is indicative of realization of the kinetic regime of aggregation wherein the rate of aggregation is limited by diffusion of the interacting particles [diffusion-limited cluster−cluster aggregation (*44*, *45*, *60*−*62*)]. In other words, each collision of the interacting particles results in their sticking together.

Previously, we showed that the power law was fulfilled for the kinetics of thermal aggregation of $\beta_L$-crystallin, glycogen phosphorylase *b* from rabbit skeletal muscle, and coat protein of tobacco mosaic virus (*35*, *53*). It is highly probable that diffusion-limited aggregation is typical of thermal aggregation of proteins.

The aggregation process includes the stage of the formation of the start aggregates and the stage of sticking together of the start aggregates (the primary clusters) and aggregates of high order. Such a pathway of aggregation results finally in the appearance of the large-sized aggregates prone to precipitation. Some authors discussed the possibility of realization of the nucleation-dependent mechanism of protein aggregation (*63*−*65*). It should be noted that if the growth of the aggregate proceeds by an attachment of the denatured protein molecule to the initial nucleus, the $R_h$ would approach a limiting value at rather high values of time as the denatured protein is depleted (*66*). Thus, data obtained in the present work show that the nucleation-dependent mechanism of protein aggregation is unlikely.

It is noteworthy that the size of the start aggregates remains constant in the temperature interval from 37 °C (the physiological temperature) to 55 °C ($R_{h,0} = 20.0 \pm 1.2$ nm). Thus, it is highly probable that the mechanism of GAPDH aggregation involving the formation of the start aggregates is operative under physiological conditions. It is surprising that at 37 °C the start aggregates appear already 50 min after the initial point of incubation. Since stability of the proteins is enhanced under the crowding conditions (*67*), one can expect that, in the cell, duration of the latent stage leading to the formation of the start aggregates will increase.

## REFERENCES


1. Fink, A. L. (1998) Protein aggregation: folding aggregates, inclusion bodies and amyloid, *Folding Dis. 3*, R9−R23.
2. Dobson, C. M. (1999) Protein misfolding, evolution and disease, *Trends Biochem. Sci. 24*, 329−332.
3. Kopito, R. R. (2000) Aggresomes, inclusion bodies and protein aggregation, *Trends Cell Biol. Biol. 10*, 524−530.
4. Bucciantini, M., Giannoni, E., Chiti, F., Baroni, F., Formigli, L., Zurdo, J., Taddei, N., Ramponi, G., Dobson, C. M., and Stefani, M. (2002) Inherent toxicity of aggregates implies a common mechanism for protein misfolding diseases, *Nature 416*, 507−511.
5. Bloemendal, H., de Jonga, W., Jaenicke, R., Lubsena, N. H., Slingsby, C., and Tardieu, A. (2004) Ageing and vision: structure, stability and function of lens crystallins, *Progr. Biophys. Mol. Biol. 86*, 407−485.
6. Markossian, K. A., and Kurganov, B. I. (2004) Protein folding, misfolding, and aggregation. Formation of inclusion bodies and aggresomes, *Biochemistry* (*Moscow*) *69*, 971−984.
7. Wickner, S., Maurizi, M. R., and Gottesman, S. (1999) Posttranslational quality control: folding, refolding, and degrading proteins, *Science 286*, 1888−1893.
8. Schulze, H., Schuler, A., Stuber, D., Dobeli, H., Langen, H., and Huber, G. (1993) Rat brain glyceraldehyde-3-phosphate dehydrogenase interacts with the recombinant cytoplasmic domain of Alzheimer's $\beta$-amyloid precursor protein, *J. Neurochem. 60*, 1915−1922.
9. Mazzola, J. L., and Sirover, M. A. (2001) Reduction of glyceraldehyde-3-phosphate dehydrogenase activity in Alzheimer's disease and in Huntington's disease fibroblasts, *J. Neurochem. 76*, 442−449.
10. Tsuchiya, K., Tajima, H., Kuwae, T., Takeshima, T., Nakano, T., Tanaka, M., Sunaga, K., Fukuhara, Y., Nakashima, K., Ohama, E., Mochizuki, H., Mizuno, Y., Katsube, N., and Ishitani, R. (2005) Pro-apoptotic protein glyceraldehyde-3-phosphate dehydrogenase promotes the formation of Lewy body-like inclusions, *Eur. J. Neurosci. 21*, 317−326.
11. Jedziniak, J. A., Arredondo, L. M., and Meys, M. (1986) Human lens enzyme alterations with age and cataract: glyceraldehyde-3-P dehydrogenase and triose phosphate isomerase, *Curr. Eye Res. 5*, 119−126.
12. Cowan-Jacob, S. W., Kaufmann, M., Anselmo, A. N., Stark, W., and Grutter, M. G. (2003) Structure of rabbit-muscle glyceraldehyde-3-phosphate dehydrogenase, *Acta Crystallogr. D59*, 2218−2227.
13. Rudolph, R., Heider, I., and Jaenicke, R. (1977) Mechanism of reactivation and refolding of glyceraldehyde-3-phosphate dehydrogenase from yeast after denaturation and dissociation, *Eur. J. Biochem. 81*, 563−570.
14. Lin, Y. Z., Liang, S. J., Zhou, J. M., Tsou, C. L., Wu, P. Q., and Zhou, Z. K. (1990) Comparison of inactivation and conformational changes of D-glyceraldehyde-3-phosphate dehydrogenase during thermal denaturation, *Biochim. Biophys. Acta 1038*, 247−252.
15. Levashov, P., Orlov, V., Boschi-Muller, S., Talfournier, F., Asryants, R., Bulatnikov, I., Muronetz, V., Branlant, G., and Nagradova, N. (1999) Thermal unfolding of phosphorylating D-glyceraldehyde-3-phosphate dehydrogenase studied by differential scanning calorimetry, *Biochim. Biophys. Acta 1433*, 294−306.
16. Muronetz, V., Kazakov, S. V., Dainiak, M. B., Izumrudov, V. A., Galaev, I., Yu. and Mattiasson, B. (2000) Interaction of antibodies and antigens conjugated with synthetic polyanions: on the way of creating an artificial chaperone, *Biochim. Biophys. Acta 1475*, 141−150.
17. Lin, Z., Wang, C., and Tsou, C. (2000) High concentrations of D-glyceraldehyde-3-phosphate dehydrogenase stabilize the enzyme against denaturation by low concentrations of GuHCl, *Biochim. Biophys. Acta 1481*, 283−288.
18. Li, J., Lin, Z., and Wang, C. C. (2001) Aggregated proteins accelerate but do not increase the aggregation of D-glyceraldehyde-3-phosphate dehydrogenase. Specificity of protein aggregation, *J. Protein Chem. 20*, 155−163.
19. Ren, G., Lin, Z., Tsou, C. L., and Wang, C. C. (2003) Effects of macromolecular crowding on the unfolding and the refolding of d-glyceraldehyde-3-phosophospate dehydrogenase, *J. Protein Chem. 22*, 431−439.
20. Velasco, P. T., Lukas, T. J., Murthy, S. N. P., Douglas-Tabor, Y., Garland, D. L., and Lorand, L. (1997) Hierarchy of lens proteins requiring protection against heat-induced precipitation by the alpha crystallin chaperone, *Exp. Eye Res. 65*, 497−505.
21. Li, J., and Wang, C. C. (1999) "Half of the sites" binding of D-glyceraldehyde-3-phosphate dehydrogenase folding intermediate with GroEL, *J. Biol. Chem. 274*, 10790−10794.
22. Lee, G. J., Roseman, A. M., Saibil, H. R., and Vierling, E. (1997) A small heat shock protein stably binds heat-denatured model substrates and can maintain a substrate in a folding-competent state, *EMBO J. 16*, 659−671.
23. Chen, Y. H., He, R. Q., Liu, Y., Liu, Y., and Xue, Z. G. (2000) Effect of human neuronal tau on denaturation and reactivation of rabbit muscle D-glyceraldehyde-3-phosphate dehydrogenase, *Biochem. J. 351*, 233−240.
24. Polyakova, O. V., Roitel, O., Asryants, R. A., Poliakov, A. A., Branlant, G., and Muronetz, V. I. (2005) Misfolded forms of glyceraldehyde-3-phosphate dehydrogenase interact with GroEL and inhibit chaperonin-assisted folding of the wild-type enzyme, *Protein Sci. 4*, 921−928.
25. Naletova, I. N., Muronetz, V. I., and Schmalhausen E. V. (2006) Unfolded, oxidized, and thermoinactivated forms of glyceraldehyde-3-phosphate dehydrogenase interact with the chaperonin GroEL in different ways, *Biochim. Biophys. Acta 1764*, 831−838.
26. Liang, S. L., Lin, Y. Z., Zhou, J. M., Tsou, C. L., Wu, P., and Zhou, Z. (1990) Dissociation and aggregation of D-glyceraldehyde-3-phosphate dehydrogenase during denaturation by guanidine hydrochloride, *Biochim. Biophys. Acta 1038*, 240−246.
27. Bettelheim, F. A., Ansari, R., Cheng, Q. F., and Zigler, J. S. Jr. (1999) The mode of chaperoning of dithiothreitol-denatured alpha-lactalbumin by alpha-crystallin, *Biochem. Biophys. Res. Commun. 261*, 292−297.
28. Schuler, J., Frank, J., Saenger, W., and Georgalis, Y. (1999) Thermally induced aggregation of human transferrin receptor studied by light-scattering techniques, *Biophys. J. 77*, 1117−1125.
29. Follmer, C., Pereira, F. V., DaSilveria, N. P., and Carlini, C. R. (2004) Jack bean urease (EC 3.5.1.5) aggregation monitored by dynamic and static light scattering, *Biophys. Chem. 111*, 79−87.

30. Militello, V., Casarino, C., Emanuele, A., Giostra, A., Pullara, F., and Leone, M. (2004) Aggregation kinetics of bovine serum albumin studied by FTIR spectroscopy and light scattering, *Biophys. Chem. 107*, 175−187.
31. Yoshida, H., Hensgens, C. M., van der Laan, J. M., Sutherland, J. D., Hart, D. J., and Dijkstra, B. W. (2205) An approach to prevent aggregation during the purification and crystallization of wild type acyl coenzyme A: isopenicillin N acyltransferase from Penicillium chrysogenum, *Protein Expression Purif. 41*, 61−67.
32. Mahler, H. C., Muller, R., Friess, W., Delille, A., and Matheus, S. (2005) Induction and analysis of aggregates in a liquid IgG1-antibody formulation, *Eur. J. Pharm. Biopharm. 59*, 407−417.
33. Hermeling, S., Schellekens, H., Maas, C., Gebbink, M. F., Crommelin, D. J., and Jiskoot, W. (2006) Antibody response to aggregated human interferon alpha2b in wild-type and transgenic immune tolerant mice depends on type and level of aggregation, *J. Pharm. Sci. 95*, 1084−1096.
34. Dusa, A., Kaylor, J., Edridge, S., Bodner, N., Hong, D. P., and Fink, A. L. (2006) Characterization of oligomers during alpha-synuclein aggregation using intrinsic tryptophan fluorescence, *Biochemistry 45*, 2752−2760.
35. Khanova, H. A., Markossian, K. A., Kurganov, B. I., Samoilov, A. M., Kleimenov, S. Yu., Levitsky, D. I., Yudin, I. K., Timofeeva, A. C., Muranov, K. O., and Ostrovsky, M. A. (2005) Mechanism of chaperone-like activity. Suppression of thermal aggregation of $\beta_L$-crystallin by α-crystallin, *Biochemistry 44*, 15480−15487.
36. Scopes, R. K., and Stoter, A. (1982) Purification of all glycolytic enzymes from one muscle extract, *Methods Enzymol. 90*, 479−490.
37. Kirschenbaum, D. M. (1972) Molar absorptivity and $A_{cm}^{1\%}$ values for proteins at elected wavelengths of the ultraviolet and visible region, *Int. J. Protein Res. 4*, 63−73.
38. Schuck, P. (2000) Size distribution analysis of macromolecules by sedimentation velocity ultracentrifugation and Lamm equation modeling, *Biophys. J. 78*, 1606−1619.
39. Brown, P. H., and Schuck, P. (2006) Macromolecular size-and-shape distributions by sedimentation velocity analytical ultracentrifugation, *Biophys. J. 90*, 4651−4661.
40. Kurganov, B. I., Kornilaev, B. A., Chebotareva, N. A., Malikov, V. Ph., Orlov, V. N., Lyubarev, A. E., and Livanova, N. B. (2000) Dissociative mechanism of thermal denaturation of rabbit skeletal muscle glycogen phosphorylase *b*, *Biochemistry 39*, 13144−13152.
41. Yudin, I. K., Nikolaenko, G. L., Kosov, V. I., Agayan, V. A., Anisimov, M. A., and Sengers, J. V. (1997) Simple photon-correlation spectrometer for research and education, *Int. J. Thermophys. 18*, 1237−1248.
42. Sanchez-Ruiz, J. M. (1992) Theoretical analysis of Lumry-Eyring models in differential scanning calorimetry, *Biophys. J. 61*, 921−935.
43. Creighton, T. E. (1993) *Proteins. Structures and Molecular Properties*, W. H. Freeman and Co, New York.
44. Weitz, D. A., Huang, J. S., Lin, M. Y., and Sung, J. (1985) Limits of the fractal dimension for irreversible kinetic aggregation of gold colloids, *Phys. Rev. Lett. 54*, 1416−1419.
45. Weitz, D. A., and Lin, M. Y. (1986) Dynamic scaling of cluster-mass distributions in kinetic colloid aggregation, *Phys. Rev. Lett. 57*, 2037−2040.
46. Díez-Orrite, S., Stoll, S., and Schurtenberger, P. (2005) Off-lattice Monte Carlo simulations of irreversible and reversible aggregation processes, *Soft Matter 1*, 364−371.
47. van Garderen, H. F., Pantos, E., Dokter, W. H., Beelen, T. P. M., and van Santen, R. A. (1994) Cluster-cluster aggregation and calculated SAXS patterns: application to concentration dependence of fractal parameters, *Modelling Simul. Mater. Sci. Eng. 2*, 295−312.
48. Sanchez-Ruiz, J. M., Lopez Lacomba, J. L., Cortijo, M., and Mateo, P. L. (1988) Differential scanning calorimetry of the irreversible thermal denaturation of thermolysin, *Biochemistry 27*, 1648−1652.
49. Lyubarev, A. E., and Kurganov, B. I. (2000) Study of irreversible thermal denaturation of proteins by the method of differential scanning calorimetry, *Usp. Biol. Khim. (Moscow) 40*, 43−84.
50. Lyubarev, A. E., and Kurganov, B. I. (2001) Study of irreversible thermal denaturation of proteins by differential scanning calorimetry, *Recent Res. Del. Biophys. Chem. 2*, 141−165.
51. Kurganov, B. I., and Agatova, A. I. (1965) Heat denaturation of lactate dehydrogenase (L-lactate:NAD-oxidoreductase, EC 1.1.1.27) and D-glyceraldehyde-3-phosphate dehydrogenase (D-glyceraldehyde-3-phosphate:NAD-oxidoreductase, EC 1.2.1.12) from rabbit muscle, *Biofizika (Moscow*) *10*, 755−762.
52. Poltorak, O. M., Chukhray, E. S., and Torshin, I. Y. (1998) Dissociative thermal inactivation, stability, and activity of oligomeric enzymes, *Biochemistry (Moscow) 63*, 303−311.
53. Markossian, K. A., Kurganov, B. I., Levitsky, D. I., Khanova, H. A., Chebotareva, N. A., Samoilov, A. M., Eronina, T. B., Fedurkina, N. V., Mitskevich, L. G., Merem'yanin, A. V., Kleymenov, S. Yu., Makeeva, V. F. Muronets, V. I., Naletova, I. N., Shalova, I. N., Asryants, R. A., Schmalhausen, E. V., Saso, L., Panyukov, Yu. V., Dobrov, E. N., Yudin, I. K., Timofeeva A. C., Muranov, K. O., and Ostrovsky, M. A. (2006) *Mechanisms of Chaperone-Like Activity, in Protein Folding: New Research* (Obalinsky, T. R., Ed.) pp 89−171, Nova Science Publishers, New York.
54. Aymard, P., Gimel, J. C., Nicolai, T., and Durand, D. (1996) Experimental evidence for a two-step process in the aggregation of beta-lactoglobulin at pH 7, *J. Chim. Phys. 93*, 987−997.
55. Le Bon, C., Nicolai, T., and Durand, D. (1999) Kinetics of aggregation and gelation of globular proteins after heat-induced denaturation, *Macromolecules 32*, 6120−6127.
56. Durand, D., Gimel, J. C., and Nicolai, T. (2002) Aggregation, gelation and phase separation of heat denatured globular proteins, *Physica A 304*, 253−265.
57. Baussay, K., Bon, L. C., Nicolai, T., Durand, D., and Busnel, J. P. (2004) Influence of the ionic strength on the heat-induced aggregation of the globular protein beta-lactoglobulin at pH 7, *Int. J. Biol. Macromol. 34*, 21−28.
58. Pouzot, M., Nicolai, T., Durand, D., and Benyahia, L. (2004) Structure factor and elasticity of a heat-set globular protein gel, *Macromolecules 37*, 614−620.
59. Turoverov, K. K., Biktashev, A. G., Khaitlina, S. Y., and Kuznetsova, I. M. (1999) The structure and dynamics of partially folded actin, *Biochemistry 38*, 6261−6269.
60. Ball, R. C., Weitz, D. A., Witten, T. A., and Leyvraz, F. (1987) Universal kinetics in reaction-limited aggregation, *Phys. Rev. Lett. 58*, 274−277.
61. Lin, M. Y., Linsday, H. M., Weitz, D. A., Ball, R. C., Klein, R., and Meakin, P. (1989) Universality of fractal aggregates as probed by light scattering, *Proc. R. Soc. London, Ser. A 423*, 71−87.
62. De Spirito, M., Brunelli, R., Mei, G., Bertani, F., Ciasca, G., Greco, G., Papi, M., Arcovito, G., Ursini, F., and Parasassi, T. (2006) LDL aged in plasma forms clusters resembling subendothelial droplets aggregation via surface sites, *Biophys. J. 90*, 4239−4247.
63. Kurganov, B. I. (2002) Estimation of the activity of molecular chaperones in test-systems based on suppression of protein aggregation, *Usp. Biol. Khim. (Moscow) 42*, 89−138.
64. Kurganov, B. I., Rafikova, E. R., and Dobrov, E. N. (2002) Kinetics of thermal aggregation of tobacco mosaic virus coat protein, *Biochemistry (Moscow) 67*, 631−640.
65. Wang, K., and Kurganov, B. I. (2003) Kinetics of heat- and acidification-induced aggregation of firefly luciferase, *Biophys. Chem. 106*, 97−109.
66. Speed, M. A., King, J., and Wang, D. J. (1997) Polymerization mechanism of polypeptide chain aggregation, *Biotechnol. Bioeng. 54*, 333−343.
67. Chebotareva, N. A., Kurganov, B. I., and Livanova, N. B. (2004) Biochemical effects of molecular crowding, *Biochemistry (Moscow) 69*, 1239−1251.

BI0610707